

## Heat transport through ion crystals

This content has been downloaded from IOPscience. Please scroll down to see the full text.

2016 Phys. Scr. 91 013007

(<http://iopscience.iop.org/1402-4896/91/1/013007>)

View [the table of contents for this issue](#), or go to the [journal homepage](#) for more

Download details:

IP Address: 157.92.4.71

This content was downloaded on 04/08/2016 at 20:44

Please note that [terms and conditions apply](#).

## Invited Comment

# Heat transport through ion crystals

Nahuel Freitas<sup>1,2</sup>, Esteban A Martinez<sup>3</sup> and Juan Pablo Paz<sup>1,2</sup><sup>1</sup> Departamento de Física, FCEyN, UBA, Ciudad Universitaria Pabellón 1, 1428 Buenos Aires, Argentina<sup>2</sup> IFIBA CONICET, UBA, FCEyN, UBA, Ciudad Universitaria Pabellón 1, 1428 Buenos Aires, Argentina<sup>3</sup> Institut für Experimentalphysik, Universität Innsbruck, Technikerstraße 25/4, 6020 Innsbruck, AustriaE-mail: [nfreitas@df.uba.ar](mailto:nfreitas@df.uba.ar)

Received 31 August 2015, revised 13 November 2015

Accepted for publication 25 November 2015

Published 16 December 2015

**Abstract**

We study the thermodynamical properties of crystals of trapped ions which are laser cooled to two different temperatures in two separate regions. We show that these properties strongly depend on the structure of the ion crystal. Such structure can be changed by varying the trap parameters and undergoes a series of phase transitions from linear to zig-zag or helicoidal configurations. Thus, we show that these systems are ideal candidates to observe and control the transition from anomalous to normal heat transport. All structures behave as ‘heat superconductors’, with a thermal conductivity increasing linearly with system size and a vanishing thermal gradient inside the system. However, zig-zag and helicoidal crystals turn out to be hyper sensitive to disorder having a linear temperature profile and a length independent conductivity. Interestingly, disordered 2D ion crystals are heat insulators. Sensitivity to disorder is much smaller in the 1D case.

Keywords: quantum thermodynamics, heat transport, ion crystals

(Some figures may appear in colour only in the online journal)

**1. Introduction**

Micro- and nano-machines [1] acting as engines and refrigerators [2] are available nowadays. These systems may be dominated by fluctuations as they operate far from the thermodynamical limit, in a regime where classical laws cannot be applied. Thus, a novel field has emerged, known as quantum thermodynamics [3, 4], focusing on the study of the emergence of thermodynamical laws as an effective description obtained from a fundamentally quantum substrate. Quantum thermodynamics also focuses on identifying the essential resources required to perform certain tasks (extract work, conduct energy, etc) in the regime where the otherwise universal laws of thermodynamics cannot be directly applied.

In this article we study energy transport through a quantum system that can be controlled to an exquisite degree: a crystal of cold trapped ions [5, 6]. Using a new approach [7, 8], that can be applied to study heat transport through general structures, we show that heat flow in ion crystals depends strongly on the crystal structure, which can be

experimentally varied. Thus, changing the trapping field or the number of ions, the crystal undergoes phase transitions that change the nature of the equilibrium state: the crystal may be a linear (1D) or a zig-zag (2D) chain, or it can have a helicoidal (3D) structure (we restrict ourselves here to study these, the simplest, cases, that have already been observed in various laboratories [5, 6]). Trapped ions are promising candidates for quantum information processing and crystals with about fifteen ions have been manipulated to create multipartite entangled states implementing small versions of quantum algorithms [9, 10]. More recently, they have been used to simulate frustrated magnetic materials and the creation of topological defects during phase transitions [11, 12]. Their potential to simulate energy flow through complex networks has also been noticed [13] and the nature of heat conduction has been recently analyzed in the most simple (linear) cases [14–16]). In particular, in [16] a toolbox of experimental techniques has been introduced to measure not only local temperatures but also the heat flow through ion crystals. This would allow phenomena such as anomalous

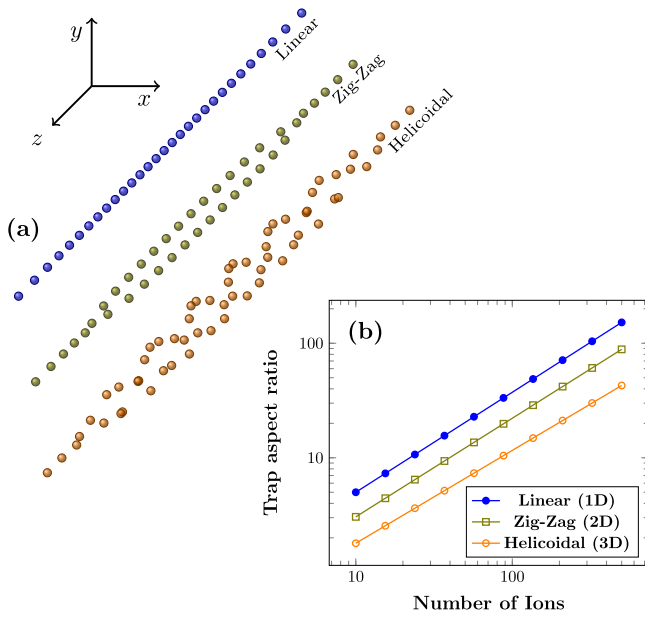


**Figure 1.** (a) Typical crystals with 30, 40 and 60 ions with one-, two- and three-dimensional structures, respectively. (b) Paths in parameter space corresponding to structures with the same order parameters (average distance to the trap axis and mean azimuthal angle between neighboring ions).

heat conduction (that is, heat conduction not following Fourier's law) to be observed in such systems. In this work we analyze heat conduction in general ion crystals using a novel analytical technique. We show that all crystals display anomalous heat transport. However, a small amount of induced disorder can control the transition to normal heat transport in 2D and 3D crystals. Thus, our results indicate that ion crystals are a promising platform to study energy transport in complex structures.

In the following section we explain the model employed to describe the dynamics of the trapped ions and the effects of their interaction with the reservoirs driving the heat flow. We also describe the method implemented to calculate the asymptotic state of the crystals.

## 2. Model and methods

We consider  $N$  ions in a Paul trap with harmonic trapping potentials both in the axial and transverse directions. The interplay between Coulomb repulsion and the trapping potentials forms crystals with variable geometries. For strong transverse confinement, the crystal is linear (1D). As the transverse potential is relaxed or the number of ions is increased the crystal undergoes a series of phase transitions. First, there is a second-order phase transition from linear (1D) to a zig-zag (2D) configuration which is followed by a transition to a helicoid (3D) and a variety of other shapes. Fully taking into account trapping potentials and Coulomb repulsion we use an evolutionary algorithm (described in the appendix) to obtain the equilibrium state of the crystal (in a regular desktop computer we can find the equilibrium state of

crystals with hundreds of ions). In figure 1 we show three different structures. Zig-zag and helicoidal structures develop at the center of the crystal and are characterized by two order parameters: the mean distance to the axis and the average azimuthal angle between ions. As shown in the figure 1(b), structures with similar order parameters are obtained by appropriately scaling the trap aspect ratio (i.e., the ratio between transverse and longitudinal trapping frequencies:  $\alpha = \omega_t/\omega_z$ ) and the number of ions  $N$  (this is explained in detail in the appendix). Once the equilibrium structure is obtained, we quantize the oscillations of the ions around equilibrium, whose dynamics are described by the Hamiltonian

$$H_S = \frac{1}{2m} P^T P + \frac{1}{2} X^T V X, \quad (1)$$

where the column vector  $X = (x_1, \dots, x_K)^T$  stores all coordinates ( $P$  stores all the momenta;  $m$  is the mass of the ions;  $K = 3N$  is the number of degrees of freedom and the superscript  $T$  denotes the transpose). The coupling matrix  $V$  arises from the second-order expansion of the full Hamiltonian. Thus, the coupling strengths depend non-trivially on the structure.

We consider that each transverse coordinate is laser cooled to two different temperatures in the left (L) and right (R) regions of the crystal, in order to induce an energy current through the crystal. In addition to these engineered reservoirs, other sources of heat could be considered. Trapped ion strings are subject to heating arising from black body radiation and RF noise, among other factors. Such mechanisms can be modeled by adding an additional thermal reservoir in contact with the whole ion string. However, for state-of-the-art traps external heating can be reduced to less than a couple of phonons per second [17, 18]. Moreover, most noise sources only contribute to heating of the center-of-mass motional modes, since typical wavelengths (larger than 1 cm for frequencies less than 30 GHz) are several orders of magnitude higher than typical ion string lengths (not more than  $\approx 100 \mu\text{m}$ ). Therefore, we will neglect external heating of the ion string in this work. Additionally, off-axis ions will be subject to micromotion coming from the trap RF fields. The effect of these fields can be incorporated into our model as an external periodic drive, which complicates the analytical solution considerably. However, without going into a full study of the effect of micromotion on the ion string, we could model its effect on heat transport as an additional source of heating owing to the factors explained in [19]. For the present treatment, we will assume that the heating due to micromotion does not affect the transport properties of the crystals.

The evolution of the motional state of a laser cooled ion in a harmonic trap satisfies a master equation which is analogous to that of a damped harmonic oscillator coupled to a finite-temperature heat bath [20]. Therefore, to model the cooling process, we couple each of the quantized transverse coordinates in the left and right regions of the crystal to two bosonic thermal baths (at temperatures  $T_L$  and  $T_R$ ). In order to describe the viscous force experienced by the ion, which is

proportional to the instantaneous velocity, we choose an Ohmic spectral density for each thermal bath. Thus, our simplified model consists of a complex network of harmonic degrees of freedom coupled to two bosonic thermal baths at different temperatures. This is a generalized version of the usual quantum Brownian motion (QBM) model which was analytically solved in [21].

The total Hamiltonian is then  $H_T = H_S + H_E + H_{\text{int}}$ , where the environmental Hamiltonian is  $H_E = \sum_l H_{E,l}$  with  $H_{E,l} = \sum_k (\pi_k^{(l)2}/2m_k + m_k \omega_k^2 q_k^{(l)2}/2)$  and the interaction is  $H_{\text{int}} = \sum_l \sum_{i,k} C_{ik}^{(l)} x_i q_k^{(l)}$  ( $q_k^{(l)}$  and  $\pi_k^{(l)}$  are the coordinate and momentum of the oscillator  $k$  of the environment  $l$ , respectively, and  $C_{ik}^{(l)}$  are coupling constants). The asymptotic state of the crystal depends only on two properties of the environments [21]: the dissipation and the noise kernels, defined as  $\gamma(\tau) = \int_0^\infty d\omega \sum_l I^{(l)}(\omega) \cos(\omega\tau)/\omega$  and  $\nu(\tau) = \hbar \int_0^\infty d\omega \sum_l I^{(l)}(\omega) \coth(\hbar\omega/(2k_B T_l)) \cos(\omega\tau)$ . The spectral density of each environment is  $I_{ij}^{(l)}(\omega) = \delta_{ij} \delta_{il} \sum_k |C_{ik}^{(l)}|^2 \delta(\omega - \omega_k)/(2m_k \omega_k)$ . We assume Ohmic environments, i.e.

$$I^{(l)} = \frac{2}{\pi} \gamma_0 P_l \frac{\omega \Lambda^2}{\Lambda^2 + \omega^2}, \quad (2)$$

where  $\Lambda$  is a high frequency cutoff,  $\gamma_0$  fixes the relaxation rate and  $P_l$  is the projector onto the coordinates in contact with the  $l$ th environment. These environments induce a friction force proportional to the velocity.

The interaction with the environment renormalizes the couplings in the system ( $V \rightarrow V_R = V - 2\gamma(0)$ ) and induces friction and diffusion, driving the system to a Gaussian stationary state. Therefore, a complete description of the asymptotic state is given by the two point correlation functions  $\langle XX^T \rangle$ ,  $\text{Re}[\langle XP^T \rangle]$  and  $\langle PP^T \rangle$ . The heat flow is obtained by computing the time derivative of the expectation value of the renormalized Hamiltonian, which is:  $d\langle H_R \rangle/dt = \text{Tr}(V_R \langle XP^T \rangle)/m$ . Then the heat current entering  $L$  (or  $R$ ) is  $\dot{Q}_{L(R)} = \text{Tr}(P_{L(R)} V_R \langle XP^T \rangle)/m$ , where  $P_L$  and  $P_R$  are projectors over the transverse coordinates of the ions in the left or right regions of the crystals. This result is intuitive: As the force on the  $i$ th coordinate is  $F_i = -(V_R X)_i$ , the expectation value of the power injected in  $i$  is  $\mathcal{P}_i = -\langle (V_R X)_i \dot{P}_i \rangle/m$ . Then, because of energy conservation we have  $\dot{Q}_i = -\mathcal{P}_i = (V_R \langle XP^T \rangle)_{ii}/m$ . Momentum correlations define the local kinetic temperature  $T_i$  through the relation  $\coth(\hbar V_{ii}^{1/2}/(2k_B T_i)) = 2\langle PP^T \rangle_{ii}/(m\hbar V_{ii}^{1/2})$ . In this way, the temperature assigned to a particular degree of freedom is the one for which the momentum dispersion of a thermal state of that same degree of freedom matches the momentum dispersion observed in the asymptotic state of the crystal. In the high temperature regime, this is simply:  $T_i = \langle PP^T \rangle_{ii}/(mk_B)$ .

The covariance matrix of the asymptotic state is well known [21, 22]. Denoting  $\sigma^{(0,0)} = \langle XX^T \rangle$ ,  $\sigma^{(1,1)} = \langle PP^T \rangle$  and

$\sigma^{(0,1)} = \text{Re}[\langle XP^T \rangle]$ , we have:

$$\sigma^{(j,k)} = \int_0^\infty d\omega (i)^{k-j} (m\omega)^{j+k} \hat{G}(i\omega) \hat{\nu}(\omega) \hat{G}(-i\omega). \quad (3)$$

Here,  $\hat{G}(s)$  is the Laplace transform of the Green's function of the system:  $\hat{G}(s) = (s^2 mI + V_R + 2s\hat{\gamma}(s))^{-1}$ , and, for an Ohmic environment,  $\hat{\gamma}(s) = \gamma_0 P_T \Lambda/(s + \Lambda)$  is the Laplace transform of the dissipation kernel ( $P_T = P_L + P_R$ ). Also,  $\hat{\nu}(\omega)$  is the Fourier transform of the noise kernel. From equation (3) it is possible to derive a integral expression for the heat flowing through the crystal in the stationary state. The following formula is obtained [21]:

$$\begin{aligned} \dot{Q} = & \pi \int_0^\infty d\omega \text{Tr} \left( I_L(\omega) \hat{G}(i\omega) I_R(\omega) \hat{G}(-i\omega) \right) \\ & \times \hbar \omega \left( \coth \left( \frac{\hbar \omega}{k_B T_A} \right) - \coth \left( \frac{\hbar \omega}{k_B T_B} \right) \right). \end{aligned} \quad (4)$$

The main ingredient to calculate the two-point correlations and the heat current in the stationary state is  $\hat{G}(s)$ , the Laplace transform of the Green's function. To compute the integrals in equations (3) and (4) several approximations and techniques are used in the literature [22]. For example, an infinite frequency cut-off is often assumed (which corresponds to a Markovian approximation, since the dissipation and noise kernels become local in time). Also, the integrals are usually evaluated numerically, which requires the inversion of  $-m\omega^2 + V_R + 2i\omega\hat{\gamma}(i\omega)$  for each evaluation point, and therefore those methods are not efficient (nor accurate) for systems with complex interactions like ion crystals.

Here, we implement a drastically different approach based on an analytic formula for  $\hat{G}(s)$ , which can be used to analytically evaluate the frequency integrals. The method is described in detail in [7, 8]. For completeness, we explain here the main ideas of the method. We consider for simplicity the high-cutoff limit (i.e.,  $\Lambda \rightarrow \infty$ ), although the method is also valid for an arbitrary cutoff. In that limit  $\hat{G}(s)^{-1} = ms^2 + V_R + 2s\gamma_0 P_T$  is a quadratic polynomial in  $s$  with matrix coefficients. Therefore, to find  $\hat{G}(s)$  it is required to invert a quadratic matrix polynomial. In analogy with the case of a regular matrix, the inverse of a quadratic matrix polynomial can be related to the eigenvalues and eigenvectors of the generalized eigenvalue problem defined by that polynomial. Explicitly, it is possible to show that  $\hat{G}(s)$  can be written as [23]:

$$\hat{G}(s) = \sum_{\alpha=1}^{2K} \frac{s_\alpha}{s - s_\alpha} r_\alpha r_\alpha^T, \quad (5)$$

where  $\{s_\alpha\}$  and  $\{r_\alpha\}$  are generalized eigenvalues and eigenvectors satisfying:

$$\hat{G}^{-1}(s_\alpha) r_\alpha = 0, \quad (6)$$

which implies  $\det(\hat{G}^{-1}(s_\alpha)) = 0$ . Since  $\det(\hat{G}^{-1}(s))$  is a  $2K$  degree polynomial in  $s$ , there are  $2K$  eigenvalues  $\{s_\alpha\}$ . Furthermore, since the matrix coefficients of  $\hat{G}^{-1}(s)$  are real, the eigenvalues and eigenvectors come in complex conjugate pairs. The Laplace transform of the Green's function  $\hat{G}(s)$  is

then expressed in terms of its poles, which are  $\{s_\alpha\}$ . In this way the integrals appearing in equations (3) and (4) can be evaluated using the residue theorem. The following result is obtained for the asymptotic covariance matrix:

$$\sigma^{(j,k)} = 2\gamma_0 \operatorname{Re} \left[ \frac{m^{j+k}}{i^{k-j+1}} \sum_{\alpha,\beta=1}^{2K} \omega_\alpha^{j+k+1} \omega_\beta \frac{r_\alpha^T A r_\beta}{\omega_\alpha + \omega_\beta} r_\alpha r_\beta^T \right], \quad (7)$$

where  $A = 2k_B \sum_l T_l P_l$ , and  $\omega_\alpha = -is_\alpha$  are the complex normal frequencies. For the heat current the result is:

$$\dot{Q} = 4\gamma_0^2 \Delta \sum_{\alpha,\beta=1}^{2K} \frac{\omega_\alpha^3 \omega_\beta}{\omega_\alpha + \omega_\beta} (r_\alpha^T P_l r_\beta) (r_\beta^T P_{l'} r_\alpha), \quad (8)$$

with  $\Delta = -2ik_B(T_L - T_R)$ . equations (7) and (8) are valid for high temperatures. Exact expressions for arbitrary temperature involving the digamma function can be found in [8]. Using equations (7) and (8), the asymptotic state and heat currents can be evaluated by simply solving a quadratic eigenvalue problem. In turn, the quadratic eigenvalue problem can be mapped to a regular (i.e., linear) eigenvalue problem by standard techniques [23] (at the price of doubling the dimension of the problem).

Surprisingly, this method has never been used to study transport in harmonic networks. In simple terms, the method provides the solution to a system of  $K$  differential equations  $m\ddot{X} + \Gamma\dot{X} + CX = 0$  for arbitrary non-commuting coupling and damping matrices  $C$  and  $\Gamma$ . In the case of spectral densities with finite frequency cutoff expressions similar to equations (7) and (8) can be derived, this time in terms of the eigenvalues and eigenvectors of a cubic eigenvalue problem [7, 8]. The method can be used to study transport phenomena in arbitrary harmonic networks, and it is thus suitable for non-trivial coupling matrices as the ones describing ion crystals, that include long-range Coulomb interactions.

### 3. Results

We now present results for ion crystal with up to  $N = 200$  ions with various structures. We use  $m$ , the mass of the ions, as the unit of mass, and  $2\pi\omega_z^{-1}$  as the unit of time. The length unit we use is given by  $l = (Q^2/(m\omega_z^2))^{1/3}$ , where  $Q$  is the electric charge of the ions (see appendix).

We analyzed the energy flow for the transverse motion and considered cases where the environment couples with single sites or with extended regions containing up to 10 percent of the crystal (no significant differences were found, in accordance with the results in [24] for the weak coupling regime). We computed the thermal conductivity  $\kappa$ , which is such that  $\dot{Q}_L = \kappa\Delta T/L$  where  $\Delta T = T_R - T_L$  and  $L$  is the length of the crystal. Fourier's law for macroscopic heat flow implies that  $\kappa$  is  $L$  independent and also temperature independent. We find that fixing  $\Delta T, \kappa$  rapidly becomes independent of the average  $\bar{T}$ . Also,  $\kappa$  becomes independent of  $\Delta T$  for moderately high values of  $\bar{T}$  (this behavior is observed for temperatures of the order of the frequencies in  $V_R/m$ ). Thus, these aspects of Fourier's law are valid. All the following results correspond to a regime in which the heat

current is proportional to  $\Delta T$ , i.e., we consider that all the normal modes are thermally excited.

However, for all structures  $\kappa$  depends linearly on the length, as shown in figure 2. This anomalous behavior is a well known property of harmonic chains [22, 25, 26] that has not yet been experimentally tested. If that behavior is extrapolated to the thermodynamic limit an infinite thermal conductivity would be obtained. Therefore, heat could be transported with the application of a vanishingly small temperature gradient. This fact, and the absence of an internal temperature gradient, which is discussed later, are reminiscent of the behavior of the electric current in superconducting materials. In [7] it is shown that in the weak coupling limit any system which is symmetric with respect to the interchange of the reservoirs (condition that is fulfilled in our model) will display a thermal conductivity increasing linearly with the size of the system. That general scaling law is not longer valid if the coupling between system and reservoirs is not small with respect to the internal couplings in the system (even if the symmetry condition still holds). Since our main interest is to study the effect of disorder on structures of different dimensionality, we restrict ourselves to the weak coupling regime (we set  $\gamma_0 = 10^{-6}$  for the numerical computations), although the method we use is valid for arbitrary coupling strength.

We show that ion crystals are ideal candidates to measure and control anomalous transport by changing the crystal structure or by adding disorder. Experimentally, disorder can be implemented in different ways. One possible approach would be to locally modify the confining potentials. However, if the potentials are to be tuned using variations in the RF confinement voltages, the electrodes have to be small enough to allow control of individual ions. The electrode size is limited by the ion-electrode spacing, and the actual state-of-the-art allows for ion-electrode spacings of  $\sim 30\text{--}40\text{ }\mu\text{m}$  [27, 28] which is larger than typical ion-ion distances of  $\sim 10\text{ }\mu\text{m}$ . Improvements in trap miniaturization might render this approach feasible in the near future. However, disorder can be implemented with the present technology using site-specific optical dipole forces. Individual ions in the ion string can be addressed with lasers to create an optical lattice with a confinement that can be tuned from site to site [16, 29].

In order to study the effects of disorder in a simple way, we numerically introduced disorder by modifying the coupling matrix  $V$  corresponding to a particular equilibrium structure. Specifically, we changed the pinning potential of  $N/2$  randomly selected ions according to the rule  $V_{ii} \rightarrow (1 \pm d)V_{ii}$ , where  $d$  is a measure of disorder. This is expected to be a qualitatively good model of particular physical realizations of disorder only for small values of  $d$ . However, values of  $d$  as small as 0.005 are enough to control the transition from anomalous to diffusive heat transport. As shown in figure 2, linear, zig-zag and helicoidal crystals display drastically different behavior as a function of disorder. Thus, zig-zag and helicoidal crystals are highly sensitive to disorder. In fact, a small  $d$  turns the zig-zag crystal into a heat insulator with  $\kappa$  rapidly approaching a vanishingly small value. The thermal conductivity of helicoidal crystals



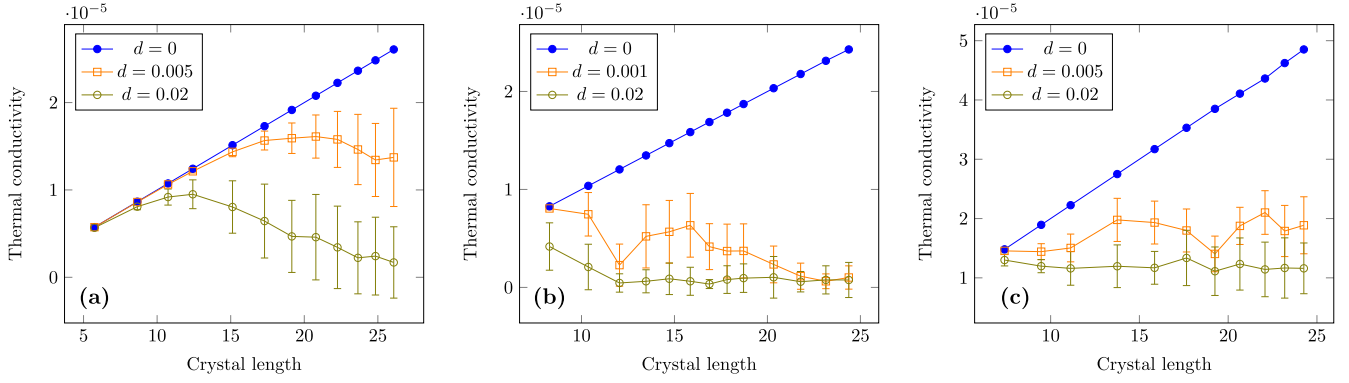


**Figure 2.** Thermal conductivity (in units of  $k_B l \omega_z$ ) as a function of crystal length and disorder for 1D linear (a), 2D zig-zag (b) and 3D helicoidal (c) structures. In all cases we considered between 20 and 200 ions. Points and error bars correspond to mean values and dispersions over several realizations of disorder.

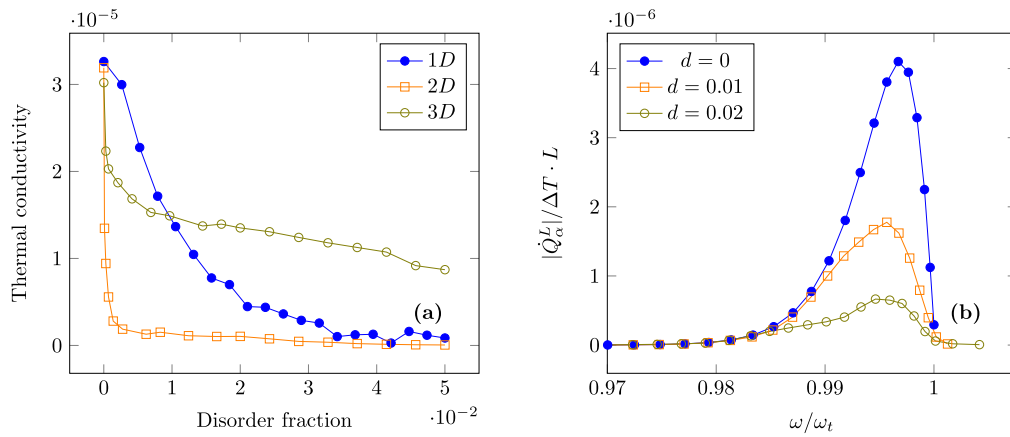


**Figure 3.** (a) Thermal conductivity versus disorder for crystals of 120 ions with different structures. (b) Contribution of each normal mode to the thermal conductivity in a 1D crystal of 100 ions.

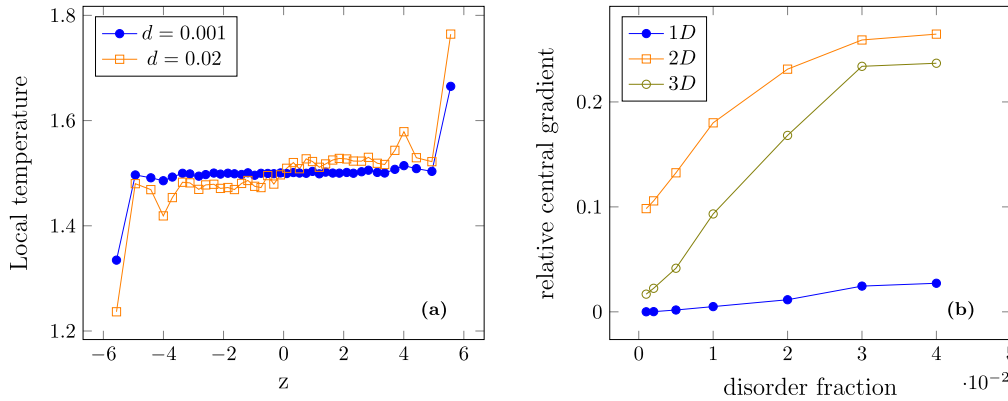


**Figure 4.** (a) Temperature profiles for a helicoidal chain of 40 ions with increasing disorder. (b) Central gradient of the temperature profile (in units of  $\Delta T / L$ ) as a function of the disorder fraction.

approaches a nonzero value for long crystals. Hypersensitivity to disorder is evident in the dependence of  $\kappa$  on  $d$  for a fixed length  $L$ . This is shown in figure 3(a) where we see that  $\kappa$  rapidly decays with  $d$  for 2D and 3D crystals. Decay for 1D crystals is clearly much slower.

We also studied the local temperature of the transverse motion. As seen in figure 4(a) the temperature profile strongly deviates from the linear behavior predicted by the classical

Fourier's law (we only show the profile for a 3D crystal but no substantial differences are seen in 1D or 2D). Without disorder the profile is almost planar except for the ions in contact with the reservoirs. As disorder is introduced, a central temperature gradient develops. Thus, deviation from Fourier's law can be measured by the central slope of the temperature profile, which is shown in figure 4(b). The central derivative strongly depends on the dimensionality: again, the

zig-zag and helicoidal crystals are hiper sensitive to disorder. For small values of  $d$  the central derivative saturates to a value which is a significant fraction of the one that correspond to a linear interpolation between the temperatures of both reservoirs.

Equations (7) and (8) enable us to estimate the contribution of each mode to thermal conductivity and temperatures. For example, the contribution of the normal mode at frequency  $\omega = \text{Re}(\omega_\alpha)$  to the heat current is:

$$\dot{Q}_\alpha = 4\gamma_0^2 \Delta \omega_\alpha^3 \sum_{\beta=1}^{2K} \frac{\omega_\beta}{\omega_\alpha + \omega_\beta} (r_\alpha^T P_I r_\beta) (r_\beta^T P_I r_\alpha). \quad (9)$$

The behavior of  $\dot{Q}_\alpha$  as a function of the mode frequency is shown in figure 3(b) for different levels of disorder. The figure shows that the largest contributions come from the modes with higher frequencies. This is expected since those are the normal modes with greater amplitude in the ends of the crystals, and therefore are the ones most coupled to the reservoirs.

#### 4. Discussion

In summary, we showed that ion crystals are excellent candidates to observe and control the transition from anomalous to normal transport. Thus, by changing the trap parameters we induce structural phase transitions which may drive the crystal to a heat insulating phase (with a zig-zag shape), which is a rather remarkable effect (evidence of the insulating properties of some idealized 2D models was presented in [22]). The toolbox presented in [16] can be used not only to measure the heat flow and local temperature but also to artificially simulate disorder. In this way, the strong dependence of thermodynamical quantities on the structure of the crystal could be observed with current technologies. To study this, we implemented a new method providing exact formulae for heat currents and temperature profiles. All these analytic (exact) results depend on generalized eigenvalues and eigenvectors of a quadratic problem (which can be easily linearized). This work was supported in part by grants from ANPCyT, UBACyT and CONICET. EAM is a recipient of a DOC Scholarship from the Austrian Academy of Sciences.

#### Appendix A. Structural phases in ion crystals

In this appendix we explain how the structural phases corresponding to 1D, 2D and 3D structures were defined. First we present details about the method used to find the equilibrium configuration of the ion crystals. We show how structural phase transitions can be determined and use them to define which are the trap parameters and number of ions needed to obtain the different structures we used.

##### A.1. Equilibrium configuration

We consider a linear Paul trap with an effective potential that is harmonic in all directions. The potential energy including

Coulomb repulsion and the effective trap potential for a system of  $N$  ions with mass  $m$  and charge  $Q$  is:

$$V = \frac{m}{2} \sum_{i=1}^N \omega_x^2 x_i^2 + \omega_y^2 y_i^2 + \omega_z^2 z_i^2 + \frac{1}{2} \sum_{i=1}^N \sum_{j \neq i}^N \frac{Q^2}{|\bar{r}_i - \bar{r}_j|}, \quad (A.1)$$

where  $\bar{r}_i = (x_i, y_i, z_i)$  is the position of the ion  $i$  measured from the minimum of the trap potential. The angular frequencies of the harmonic potential are  $\omega_x$ ,  $\omega_y$  and  $\omega_z$ . We rewrite the energy in terms of the parameters  $\alpha_x = \omega_x/\omega_z$ ,  $\alpha_y = \omega_y/\omega_z$  and  $q^2 = Q^2/(m\omega_z^2)$ :

$$V = \frac{m\omega_z^2}{2} \sum_{i=1}^N \left( \alpha_x^2 x_i^2 + \alpha_y^2 y_i^2 + z_i^2 + \sum_{j \neq i}^N \frac{q^2}{|\bar{r}_i - \bar{r}_j|} \right). \quad (A.2)$$

It is clear from this expression that the equilibrium configuration of the  $N$  ions will only depend on the parameters  $N$ ,  $\alpha_x$ ,  $\alpha_y$  and  $q$ . We will only consider the case of a trap with cylindrical symmetry, i.e.,  $\alpha_x = \alpha_y = \alpha$ . A length scale is fixed by setting  $q^2 = 1$ . Thus, the equilibrium structure is completely determined by  $N$  and  $\alpha$ , apart from a scaling in the position of all the ions (this scaling can be performed by varying  $\omega_z$  while keeping  $\alpha$  to a constant value).

The determination of  $3N$  coordinates  $\{(x_i, y_i, z_i)\}$  that correspond to a global minimum of the energy is a hard problem that even for small values of  $N$  can only be treated numerically. A typical approach to find a global minimum would be to use some gradient-descent algorithm combined with some strategy to avoid local minima. We decided to use a simpler solution based on the differential evolution algorithm [30]. This algorithm does not use gradient information, although it can be taken into account in a very simple way to improve both convergence and the quality of the solution. This method enable us to determine equilibrium configurations of crystals with more than 200 ions (600 degrees of freedom) in a modest personal computer.

As is well known, the ion crystals studied here present structural phase transitions as the trap parameters or the number of ions are changed [5]. We will use these phase transitions to define ‘structural phases’ in the parameter space spawned by  $\alpha$  and  $N$ . As an example, figure 5(a) shows the transition from a 1D linear configuration to a 2D zig-zag configuration in a chain of 30 ions as the transverse trapping potential is relaxed ( $\alpha$  is decreased). In this case the order parameter is the chain radius defined as  $R = \max_{1 \leq i \leq N} \{\sqrt{x_i^2 + y_i^2}\}$ . In a similar way it is possible to measure the transition from 2D configurations to 3D helical configurations [5]. Another phase transition occurs if the trap aspect ratio continues to decrease: beyond some point, the ions in the equilibrium configuration can no longer be ordered according to their  $z$  coordinate, i.e.,  $z_i \simeq z_j$  for one or more pairs of ions. It is possible to detect this phase transition by measuring the order parameter  $\Delta = \min_{1 \leq i, j \leq N (i \neq j)} \{|z_i - z_j|\}$ , as shown in figure 5(b).

The transition points for chains with different numbers of ions are shown in figure 6. As noted in [5], the relation of the critical values of  $\alpha$  with the number of ions is well approximated (for  $N > 20$ ) by a simple power law:  $\alpha_c \propto N^\beta$ . We

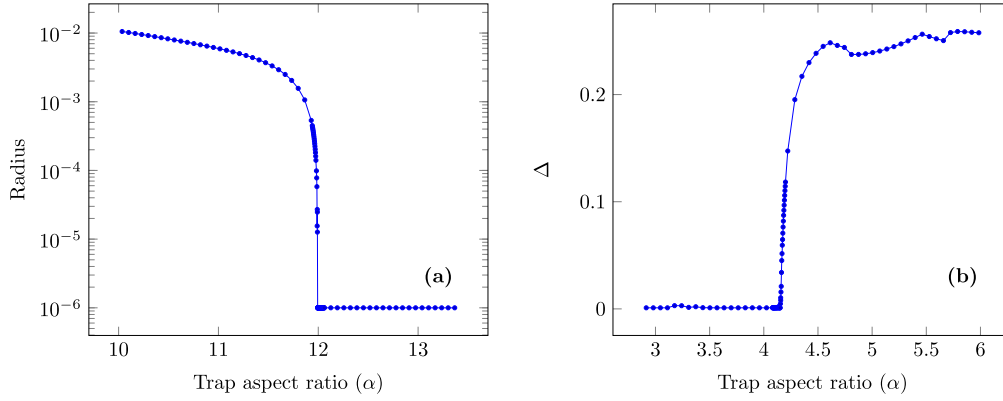


**Figure 5.** (a) Radius of a chain of 30 ions as the trap aspect ratio is decreased. Transition from 1D to 2D structures. (b) Minimum longitudinal separations of the ions ( $\Delta$ ) as the aspect ratio is decreased.

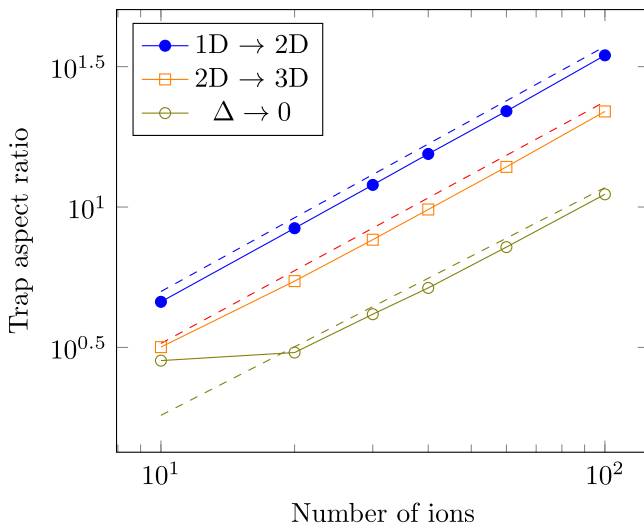


**Figure 6.** Transition points for several numbers of ions.

**Table 1.** Coefficients of the power laws used to generate crystal structures of different dimensionality.

	$c$	$\beta$
1D	0.67	0.873
2D	0.44	0.861
3D	0.28	0.811

estimated the exponent  $\beta$  for each transition. Therefore, we can define power laws  $\alpha = cN^\beta$  with the same exponent  $\beta$  but choosing  $c$  so that the power laws are sub-critical. The resulting power laws are shown with dashed lines in figure 6. These paths in parameter space define ‘structural phases’, in the sense that they determine a family of crystals with similar structural properties. In table 1 we give the values of  $c$  and  $\beta$  we used to generate 1D, 2D and 3D structures with different number of ions.

## References

- [1] Cerefolini G 2009 *Nanoscale Devices: Fabrication, Functionalization, and Accessibility from the Macroscopic World* (New York: Springer)
- [2] Abah O, Rossnagel J, Jacob G, Deffner S, Schmidt-Kaler F, Singer K and Lutz E 2012 Single-ion heat engine at maximum power *Phys. Rev. Lett.* **109** 203006
- [3] Gemmer J, Michel M and Mahler G 2009 *Quantum Thermodynamics. Emergence of Thermodynamic Behavior Within Composite Quantum Systems* (Lecture Notes in Physics) (New York: Springer)
- [4] Kosloff R 2013 Quantum thermodynamics: a dynamical viewpoint *Entropy* **15** 2100–28
- [5] Schiffer J P 1993 Phase transitions in anisotropically confined ionic crystals *Phys. Rev. Lett.* **70** 818
- [6] Morigi G and Fishman S 2004 Eigenmodes and thermodynamics of a Coulomb chain in a harmonic potential *Phys. Rev. Lett.* **93** 170602
- [7] Freitas N and Paz J P 2014 Analytic solution for heat flow through a general harmonic network *Phys. Rev. E* **90** 042128
- [8] Freitas N and Paz J P 2014 Analytic solution for heat flow through a general harmonic network *Phys. Rev. E* **90** 042128
- [9] Freitas N and Paz J P 2014 *Phys. Rev. E* **90** 069903 (erratum)
- [10] Häffner H *et al* 2005 Scalable multiparticle entanglement of trapped ions *Nature* **438** 643–6
- [11] Blatt R and Wineland D 2008 Entangled states of trapped atomic ions *Nature* **453** 1008–15
- [12] Islam R, Senko C, Campbell W C, Korenblit S, Smith J, Lee A, Edwards E E, Wang C-CJ, Freericks J K and Monroe C 2013 Emergence and frustration of magnetism with variable-range interactions in a quantum simulator *Science* **340** 583–7
- [13] Pyka K *et al* 2013 Topological defect formation and spontaneous symmetry breaking in ion Coulomb crystals *Nat. Commun.* **4** 2291
- [14] Pruttivarasin T, Ramm M, Talukdar I, Kreuter A and Häffner H 2011 Trapped ions in optical lattices for probing oscillator chain models *New J. Phys.* **13** 075012
- [15] Lin G D and Duan L M 2011 Equilibration and temperature distribution in a driven ion chain *New J. Phys.* **13** 075015
- [16] Manzano D, Tiersch M, Asadian A and Briegel H J 2012 Quantum transport efficiency and fourier’s law *Phys. Rev. E* **86** 061118
- [17] Bermudez A, Bruderer M and Plenio M B 2013 Controlling and measuring quantum transport of heat in trapped-ion crystals *Phys. Rev. Lett.* **111** 040601
- [18] Labaziewicz J, Ge Y, Antohi P, Leibbrandt D, Brown K R and Chuang I L 2008 Suppression of heating rates in cryogenic surface-electrode ion traps *Phys. Rev. Lett.* **100** 013001



- [18] Niedermayr M, Lakhmanskiy K, Kumph M, Partel S, Edlinger J, Brownnutt M and Blatt R 2014 Cryogenic surface ion trap based on intrinsic silicon *New J. Phys.* **16** 113068
- [19] Wineland D J, Monroe C, Itano W M, Leibfried D, King B E and Meekhof D M 1997 Experimental issues in coherent quantum-state manipulation of trapped atomic ions arXiv:quant-ph/9710025
- [20] Cirac J I, Blatt R, Zoller P and Phillips W D 1992 Laser cooling of trapped ions in a standing wave *Phys. Rev. A* **46** 2668
- [21] Martinez E A and Paz J P 2013 Dynamics and thermodynamics of linear quantum open systems *Phys. Rev. Lett.* **110** 130406
- [22] Chaudhuri A, Kundu A, Roy D, Dhar A, Lebowitz J L and Spohn H 2010 Heat transport and phonon localization in mass-disordered harmonic crystals *Phys. Rev. B* **81** 064301
- [23] Tisseur F and Meerbergen K 2001 The quadratic eigenvalue problem *SIAM Rev.* **43** 235–86
- [24] Velizhanin K A, Chien C-C, Dubi Y and Zwolak M 2013 Intrinsic thermal conductance, extended reservoir simulations, and Kramers transition rate theory arXiv:1312.5422
- [25] Dhar A 2008 Heat transport in low-dimensional systems *Adv. Phys.* **57** 457–537
- [26] Lepri S, Livi R and Politi A 2003 Thermal conduction in classical low-dimensional lattices *Phys. Rep.* **377** 1–80
- [27] Stick D, Hensinger W K, Olmschenk S, Madsen M J, Schwab K and Monroe C 2006 Ion trap in a semiconductor chip *Nat. Phys.* **2** 36–9
- [28] Seidelin S *et al* 2006 Microfabricated surface-electrode ion trap for scalable quantum information processing *Phys. Rev. Lett.* **96** 253003
- [29] Enderlein M, Huber T, Schneider C and Schaetz T 2012 Single ions trapped in a one-dimensional optical lattice *Phys. Rev. Lett.* **109** 233004
- [30] Storn R and Price K 1997 Differential evolution—a simple and efficient heuristic for global optimization over continuous spaces *J. Glob. Optim.* **11** 341–59